A construction robot path planning method based on safe space and worker trajectory prediction

Xiaotian Ye[1], Hongling Guo[1, *], Ziyang Guo[1], Zhubang Luo[1]

[1]Department of Construction Management, Tsinghua University, Beijing, China
yxt19@mails.tsinghua.edu.cn, hlguo@tsinghua.edu.cn, ziyangguo@mail.tsinghua.edu.cn, lzb2017@mail.tsinghua.edu.cn

Abstract –

As the key to intelligent construction, construction robots can perform complex and dangerous tasks instead of workers. Construction robot path planning (CRPP) is a prerequisite for executing tasks. However, dynamic environments and moving workers at sites create significant difficulties for CRPP. To solve this issue, this research proposes a construction robot path planning method based on safe space and worker trajectory prediction. Firstly, a grid map with a target point is automatically established based on BIM (Building Information Modeling) and construction schedule. Secondly, an improved A* algorithm with a dynamic weight of the heuristic function is developed for global path planning. Thirdly, the worker and robot safe space are defined, and worker trajectory is predicted to improve the DWA (Dynamic Window Approach) for local path planning. Furthermore, a decision model is developed to deal with the path conflict based on the potential collision zone (PCZ). Finally, an experiment is designed and conducted to validate the proposed method. It is found that the method can effectively achieve the optimal path and resolve path conflict to ensure worker and robot safety.

Keywords –

Construction robot path planning; Safe space; Worker trajectory prediction; Decision model.

1 Introduction

The construction industry contributes to economic growth worldwide and boosts numerous countries' gross domestic product. However, it is confronted with global challenges, such as labour shortages, stagnant productivity, and frequent safety incidents [1]. An MGI (McKinsey Global Institute) survey indicates that over the past 20 years, the annual growth rate of labour productivity in the construction industry has been a mere 2%, significantly lagging behind other industries [2]. Construction robots and automation technologies are recognized as the key to enhancing construction efficiency and safety [3]. Construction robots have demonstrated their advantages in various fields, including main structure and decoration works [4], building cleaning and waste recycling [5], and structural inspection.

In construction environment, safe and efficient path planning is not only the fundamental to the execution of construction tasks by robots but also a critical factor in enhancing their operation efficiency [6]. The continuous dynamic changes at construction sites, especially the uncertainty caused by workers and machinery, pose enormous challenges to their collaboration safety while accomplishing their tasks [7]. Therefore, it is urgent to improve construction robots' path-planning capability at construction sites.

Related advancements have been made in robotic path planning within construction scenarios. Pinto et al. developed a Vision-Guided Path-Planning System (V-GPP). The system employs RGB-D cameras to acquire real-time environmental data, integrating A* algorithm and 3D grid maps to plan safe routes for cable-driven robots [8]. Do et al. [9] utilized depth cameras to collect information about onsite environment and obstacles, refining the path planning of sTetro robots for stair-cleaning tasks through grid optimization and heat conduction analysis. However, current research mainly involves dynamic obstacles whose information is known and indoor scenarios, and ignores path conflict resolution strategies for random dynamic entities on site, especially in effectively integrating worker trajectory prediction with robotic path planning.

Therefore, this research proposes a dynamic path-planning method considering safe space and predicted worker trajectory to ensure the safety of worker-robot collaboration. A literature review is first made in Section 2. Then, the path planning method is illustrated in Section 3 and an experiment is conducted to test its performance in Section 4. In the end, a conclusion is drawn in Section 5.

2 Literature review

2.1 Path planning in dynamic environments

Path planning-related research primarily focuses on global path planning based on known information and local path planning based on real-time sensor feedback.

Global path planning can find the optimal route by fully exploiting the existing scene knowledge in static environments. Graph-search-based algorithms such as A* [10] and D* [11] have been extensively applied in path planning. Furthermore, biomimetic heuristic algorithms such as GA (Genetic Algorithm) [12], ACO (Ant Colony Optimization) [13], and neural network algorithms [5] have provided new perspectives for robotic path planning. By introducing a heuristic function, A* algorithm has significant advantages in enhancing search efficiency and is considered the best-first algorithm [14].

Local path planning is crucial in guiding robots to avoid dynamic obstacles. The most used local path planning algorithms include Artificial Potential Field (APF) [15], Dynamic Window Approach (DWA) [16], and reinforcement learning-based method [17,18]. For instance, Anirudh et al. [17] trained a Coverage Path Planning (CPP) model for a tile-laying robot using reinforcement learning, maximizing the area coverage of tile laying while minimizing energy consumption.

To address path planning problems in dynamic environments, a hybrid strategy that integrates global and local path planning has received significant attention. The hybrid approach initially generates an optimal route based on global path planning and then makes flexible adjustments using local path planning [19]. However, the method overlooks trajectory prediction for dynamic obstacles and fails to consider the safe space of workers and robots. Most studies expand on obstacles but lack a comprehensive and effective solution for path conflict.

2.2 Worker trajectory prediction

The dynamic and random environment of construction sites leads to frequent safety incidents [20] and poses significant challenges to construction robot path planning. The predicted trajectories of workers and machinery can enhance the efficiency and safety of path planning in such environments[21]. In current studies, trajectory prediction methods are primarily categorized into physics-based approaches (Sense - Predict) and learning-based approaches (Sense - Learn - Predict) [22].

Physics-based approaches are based on dynamic or kinematic models, using mathematical formulas to depict target motion. Zhu et al. utilized a Kalman filter to integrate parameters such as position, velocity, and acceleration for predicting the locations of workers and mobile equipment [23]. Considering the randomness of worker movement, some studies have adopted Markov Models to forecast workers' potential trajectories and statuses [24,25]. The parameters of these models are derived from historical data and do not require training data, which are suited for short-term predictions.

Learning-based approaches can extract dynamic models and statistical behaviour patterns from vast training data, thus allowing long-term predictions in complex and dynamic environments. Long Short-Term Memory (LSTM) networks have been commonly used for motion trajectory prediction. Tang et al. [26,27] developed an LSTM encoder-decoder and combined it with a Mixture Density Network (MDN) to model the uncertainty in predictions, achieving entity trajectory forecasting up to 2 seconds. Cai et al. [28] proposed a context-aware LSTM-based method, extracting abundant contextual information (e.g., neighbour position, the relationship with the neighbour, and the distance from the destination) and feeding these data into the LSTM model for precise worker trajectory prediction.

Learning-based approaches rely on extensive historical data while acquiring high-quality data at construction sites is challenging. This limits the accuracy of the models. On the other hand, physics-based approaches do not rely on massive historical data, which is more suitable for construction environments.

3 Path planning method

This method involves map establishment, global path planning, local path planning, and decision-making. This research establishes a grid map based on the BIM (Building Information Modeling) model and construction schedule, develops an improved A* algorithm for global path planning in the static map and an improved DWA for local path planning based on safe space and predicted worker trajectory, and builds a decision model to reduce unnecessary local planning.

3.1 BIM-based map establishment

BIM includes plenty of building information, which can provide a basis for establishing construction maps. By exporting a BIM model to an IFC (Industry Foundation Classes) file, basic information such as component type, component location, and geometric dimensions, can be extracted to generate a preliminary map. The IFC has a standard syntax to obtain component-related information. For example, IFCCARTESIANPOINT in Figure. 1(b) represents the position of a column, and IFCCOLUMNTYPE contains the component's global ID (e.g. the column's global ID is '1I2u_TieX4cg$DLo1NNHAJ') and its attribute information such as the component type and dimensions (e.g. the component type is COLUMN and its cross-section size is 500x500mm). With the location and cross-

section information, each component can be drawn in the grid map. Meanwhile, the construction schedule is automatically generated based on previous research by the authors [29] (e.g., Figure. 1(c)). Both completed construction tasks and those to be completed can be obtained from the schedule to update the grid map (e.g., Figure. 1(d)). Each gray rectangle not only represents an obstacle but also has semantic information (e.g., component type and size) through the global ID. The gray rectangles represent the columns that have been constructed, while the red one represents the column to be done, which is the target for the construction robot.

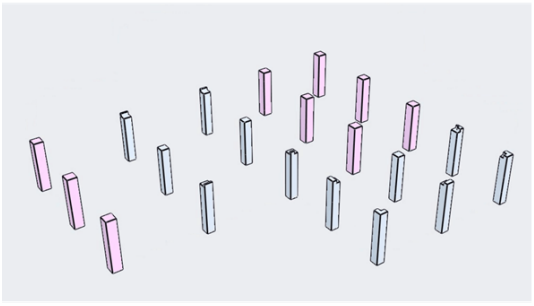

(a) BIM model

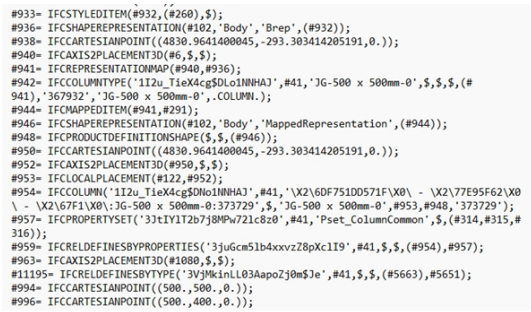

(b) IFC file

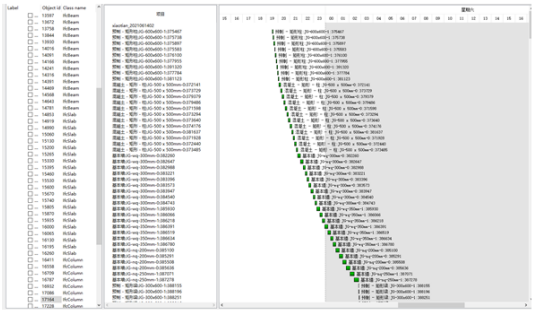

(c) Construction schedule

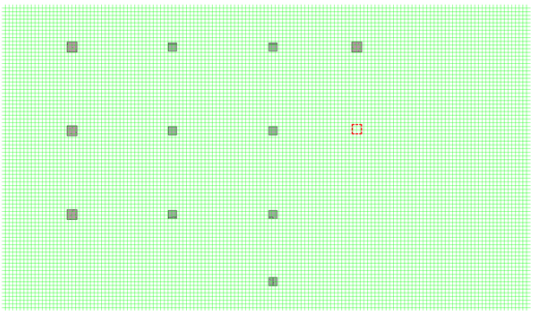

(d) Grid map with a schedule

Figure 1. The establishment of a grid map

3.2 Improved A* for global path planning

A* algorithm is a heuristic search algorithm suitable for global path planning in a static environment with known information. The basic idea is to sort the cost of the optional nodes around a current node, select the least-cost node, and repeat the process until it reaches the target point. In a 2D grid map, A* algorithm utilizes the cost function f(n) to evaluate the path length as Equation (1).

$$\mathrm{f(n)} = g(n) + h(n) \quad (1)$$

Where, $g(n)$ is the distance from the start node to the current node, and $h(n)$ is the heuristic function representing the distance from the current node to the destination.

Traditional A* algorithms use the same weights for $g(n)$ and $h(n)$, which leads to more search nodes and low efficiency. This research adds dynamic weight w to $h(n)$ (see Equation (2)), increasing w when $g(n)$ is less than $h(n)$ and decreasing w when $g(n)$ is greater than $h(n)$. The dynamic weight can consider the characteristics of the construction schedule to reduce the search space and increase the search speed.

$$\mathrm{f(n)} = g(n) + w \cdot h(n) \quad (2)$$

3.3 Improved DWA for local path planning

In traditional DWA, robots' speed limit only considers motor performance and braking distance. Besides, the distance and velocity functions are built based solely on the simple expansion of an obstacle. The dynamic properties of robots and workers and the future state of workers are not considered. Therefore, a safe space is defined and created for both workers and robots, and worker trajectory is predicted to modify DWA to ensure the safety of the path.

3.3.1 Safe space definition of workers and robots

(1) Worker safe space

This research defines worker safe space (WSS) as the worker operation space (WOS) and worker movement space (WMS), as shown in Figure. 2. WOS refers to the maximum space occupied by a worker's operation. This research adopts the maximum arm span of a standing worker as WOS, which is a circle with radius r_w. According to Chinese National Standard GB/T 13549-92 "Human dimensions in workspace" [30], the arm span of an adult male is 1.78m (90th percentile). WMS is the distance s_w traveled by a worker during the period of time when a robot detects the worker and reacts until the robot comes to a complete stop. WOS is a static region, while WMS is dynamic and related to worker speed.

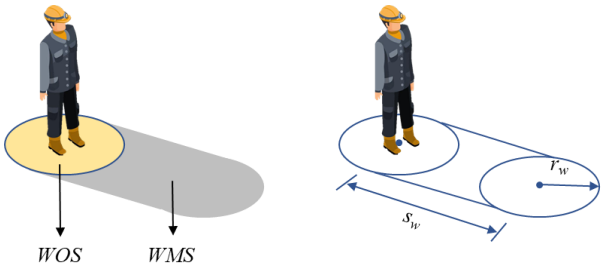

Figure 2. Worker safe space

Referring to ISO 15066 [31], s_w is calculated as Equation (3).

$$s_w = \int_{t_0}^{t_0+T_r+T_s} v_w(t)\,dt \tag{3}$$

Where, t_0, T_r, T_s represent the present time, the reaction time of a construction robot, and the stopping time of the robot; v_w is the worker's speed in the direction of the robot. ISO 13855 [32] recommends a value of 1.6 m/s for the speed of human motion, thus Equation (3) can be simplified to Equation (4).

$$S_w = v_w(T_r + T_s) = 1.6 \times (T_r + T_s) \tag{4}$$

(2) Construction robot safe space

This research defines construction robot safe space (CRSS), which consists of self-occupied space (SS), safety distance (SD), and braking space (BS) (see Figure. 3). SS is the smallest outer circle occupied by a robot. SD refers to the minimum distance l_{cr} that should be maintained between a worker and the robot in a collaborative situation. According to ISO10128 [33], l_{cr} takes the value of 0.5m. BS means the distance s_{cr} traveled by the robot from the time point to detect the worker to that to stop.

As in Equations (5) and (6), s_{cr} consists of s_{cr1} and s_{cr2}. s_{cr1} represents the distance traveled during the reaction time of the robot, while S_{cr2} represents the distance travelled during the robot's stopping time.

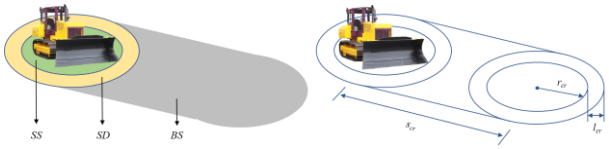

Figure 3. Construction robot safe space

$$S_{cr1} = \int_{t_0}^{t_0+T_r} v_r(t)\,dt \tag{5}$$

$$S_{cr2} = \int_{t_0+T_r}^{t_0+T_r+T_s} v_s(t)\,dt \tag{6}$$

Where, v_r is the directed speed of the robot in the direction of the worker. v_s is the speed of the robot in the course of stopping. In this research, the robot's motion during the reaction time is simplified as a uniform velocity motion, and the motion during the stopping time is simplified as a constant deceleration motion. Then, Equations (5) and (6) are respectively simplified to Equations (7) and (8).

$$S_{cr1} = v_r(t_0) \times T_r \tag{7}$$

$$S_{cr2} = \frac{1}{2} v_r(t_0) T_s \tag{8}$$

With the safe space of workers and robots, the objective functions (e.g., distance and velocity) can be optimized in DWA algorithm.

3.3.2 Worker trajectory prediction

In the context of intelligent construction, construction robots are disturbed mainly by workers and other robots on site. This paper assumes that construction robots onsite can interact with each other to avoid collisions, which can reduce some unpredictable interference. Construction workers are the most common and complex dynamic obstacles at construction sites. Therefore, this study focuses on the worker as a dynamic obstacle for localized collision avoidance. Predicting worker trajectory can provide abundant information for the local path planning of robots and improve their path safety. Differing from the traditional prediction that assumes an obstacle to move in a uniform linear motion, this research considers worker turning and establishes a nonlinear model of workers (i.e., constant linear velocity v and angular velocity ω). Then, worker trajectory is predicted based on CKF (Cubature Kalman Filter). The status vector ψ is defined as Equations (9) and (10).

$$\psi = \begin{bmatrix} x \\ y \\ v \\ \theta \\ \omega \end{bmatrix} \tag{9}$$

$$\psi_t = \psi_{t-1} + \int_{t-1}^{t} \begin{bmatrix} x'(t) \\ y'(t) \\ v'(t) \\ \theta'(t) \\ \omega'(t) \end{bmatrix} dt \begin{bmatrix} x_{t-1} + \frac{v}{\omega} sin\theta_{t-1} \cos(\omega * \Delta t) + \frac{v}{\omega} cos\theta_{t-1} \sin(\omega * \Delta t) - \frac{v}{\omega} sin\theta_{t-1} \\ y_{t-1} - \frac{v}{\omega} cos\theta_{t-1} \cos(\omega * \Delta t) + \frac{v}{\omega} sin\theta_{t-1} \sin(\omega * \Delta t) + \frac{v}{\omega} cos\theta_{t-1} \\ \theta_{t-1} + \omega * \Delta t \end{bmatrix} \quad (10)$$

Where, x, y, v, θ and ω denote the horizontal coordinates, vertical coordinates, velocity, angle, and the deflection angular velocity of a worker at time t, respectively.

The status and observation equations are defined as Equations (11) and (12), respectively.

$$\psi_t = F(\psi_{t-1}) + \varphi_t \quad (11)$$

$$Z_t = \mathrm{H} * \psi_t + \lambda_t \quad (12)$$

Where, F, φ_t, Z_t, H, and λ_t is the nonlinear status transition matrix, the system noise vector, the observation vector, the observation matrix, and the observation noise vector, respectively. The observation vector Z can be obtained by collecting worker coordinates from sensors. The observation matrix H in Equation (14) shows the transformation from the state vector ψ_t to the observation vector Z_t.

$$Z = \begin{bmatrix} x \\ y \end{bmatrix} \quad (13)$$

$$H = \begin{bmatrix} 1 & 0 & 0 & 0 & 0 \\ 0 & 1 & 0 & 0 & 0 \end{bmatrix} \quad (14)$$

φ_t and λ_t are assumed to satisfy positive definite, symmetric and uncorrelated, zero mean Gaussian white noise vector, e.g., $\varphi_t \sim N(0, Q_t)$, $\lambda_t \sim N(0, R_t)$ in Equation (15) and (16).

$$Q = \begin{bmatrix} \sigma_x & 0 & 0 & 0 & 0 \\ 0 & \sigma_y & 0 & 0 & 0 \\ 0 & 0 & \sigma_v & 0 & 0 \\ 0 & 0 & 0 & \sigma_\theta & 0 \\ 0 & 0 & 0 & 0 & \sigma_\omega \end{bmatrix} \quad (15)$$

$$R = \begin{bmatrix} \sigma_{x'} & 0 \\ 0 & \sigma_{y'} \end{bmatrix} \quad (16)$$

Where, σ_x, σ_y, σ_v, σ_θ, and σ_ω represent the variances of x, y, v, θ, and ω respectively. $\sigma_{x'}$ and $\sigma_{y'}$ respectively represent the variances of the observation vector. The status vector ψ includes 5 parameters belonging to a high dimensional system. For nonlinear state estimation, Arasaratnam and Haykin [34] proposed the CKF, which derives a third-degree spherical-radial cubature rule. The aforementioned kinematic model belongs to the nonlinear state model, solved using CKF. Then, the predicted trajectory can optimize the DWA's distance function and velocity range. Meanwhile, considering some unpredictable disturbances onsite, we shorten the exploration time (i.e., the search step of DWA) to minimize collisions in the search space.

3.4 A decision model for path conflict

Path conflict is the core of the dynamic planning problem. However, a path conflict does not mean that a collision will occur. Collisions happen when both spatial and temporal conflicts occur. Therefore, to reduce unnecessary local planning and make path planning more efficient, a decision model is proposed. Based on the global path and worker trajectory prediction, the potential collision zone (PCZ) between the paths can be obtained to determine if spatial conflicts occur (see Figure. 4). The PCZ is generated and updated in real time since the worker trajectory is predicted in real-time. If there are no PCZs between the two paths, there will be no spatial conflicts between the worker and the robot. Therefore, collisions do not occur, and the robot can follow the globally optimal path.

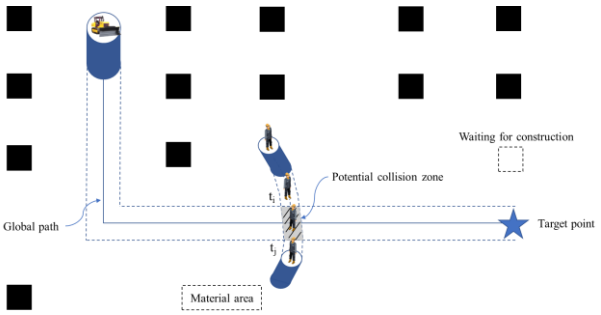

Figure 4. Potential collision zone (PCZ)

When a PCZ exists (i.e., a spatial conflict exists), the decision model will further determine the temporal conflict to select a decision. The time for workers to enter and leave the PCZ is calculated as t_i and t_j respectively. Then, the time for the construction robot to enter and leave the PCZ is calculated as t_p and t_q. Depending on the time when the robot enters the PCZ, the following robot decisions are made: 1) Maintain the original speed and path, 2) Maintain the original path and reduce speed, and 3) Change paths. The decision model is presented as follows:

Case 1: When $t_q < t_i$, the worker has crossed the PCZ, while the robot has not yet entered the PCZ. Therefore, the robot can travel at its original path and speed.

Case 2: When $t_p > t_j$, the worker has not yet entered the PCZ, while the robot has crossed the PCZ. Therefore, the robot can travel on its original route and speed.

Case 3: When $t_p < t_i < t_q < t_j$ and $t_p < t_i < t_j < t_q$,

the robot and the worker will meet in the PCZ, with the robot entering the PCZ first. Therefore, the robot needs to change a path locally.

Case 4: When $t_i < t_p < t_q < t_j$ and $t_i < t_p < t_j < t_q$, the robot and the worker will meet in the PCZ, with the worker entering the PCZ first. Therefore, the robot needs to reduce speed or change paths. If the robot cannot avoid the collision by decelerating, the robot needs to change path locally.

A sudden turn by the worker can lead to a failed trajectory prediction, in which case the decision model will control the robot to stop immediately (e.g. decision (2)). The improved DWA will plan a local path for these cases, where changing paths is required. The decision model reduces robot replanning and unnecessary local planning, allowing the robot to follow the optimal path as much as possible.

4 Experiment and test

4.1 Experiment

An experiment was designed to validate the feasibility of the proposed method. For global path planning, the experiments tested the improved A* algorithm on a grid map with a schedule (see Figure 5). In the grid map, the left side represents completed construction areas, and the right side represents areas that have not yet started. For local path planning, the test used a tracked vehicle to represent a construction robot and a humanoid robot to represent a worker, as shown in Figure. 6. Meanwhile, columns and materials were placed in the scene to simulate a construction site better.

A depth camera was utilized to acquire the position of the worker and robot, further calculating their safe spaces, and predicting worker trajectories. Then, the improved A* algorithm was utilized to plan the global path. As a dynamic obstacle, the worker moved at different speeds within a low-speed range and conflicted with the global path. Based on the decision model, the construction robot would decide whether to perform local path planning.

4.2 Results

The improved A* can successfully generate the global path as shown in Figure. 5. Meanwhile, table 1 compares the planning time of traditional and improved A* algorithms under various starting and target points. In the local path planning scenario, the global path (the purple line) and the predicted worker trajectory (the blue band) are shown in Figure. 6. A PCZ exists between the global path and the predicted trajectory. In Figure. 6, since the worker would leave before the robot reached the PCZ, the robot followed its original path and speed without local path planning according to the decision model. In Figure. 7, the robot and the worker would meet in the PCZ, where the path needs to be locally planned using the improved DWA algorithm. Figure. 7 (a) shows the local path (the blue line) considering the predicted worker trajectory. The robot found a path behind the worker, preventing the secondary collision from going around in front of the worker. Compared with the local path without the prediction in Figure. 7 (b), the robot passed in front of the worker, which might cause a secondary collision.

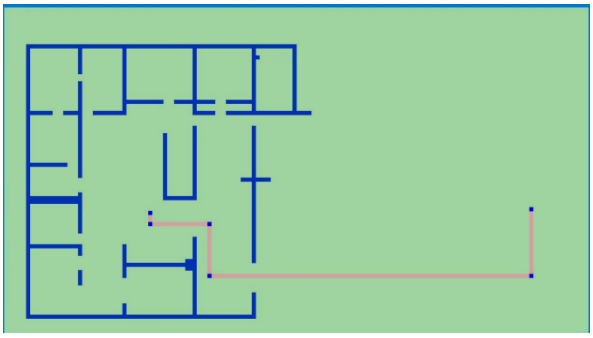

Figure 5. The experimental scenario for global path planning

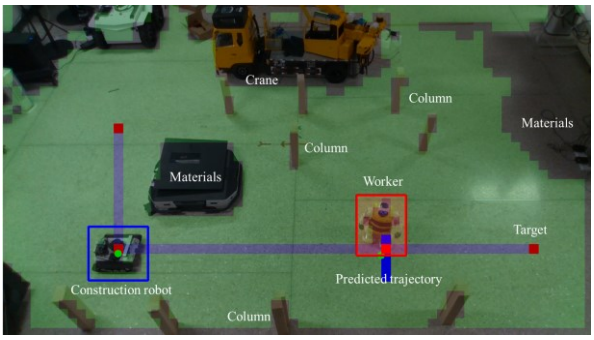

Figure 6. The experimental scenario for local path planning

Table 2 presents the comparison of prediction results for the worker and decisions for the robot with and without a sudden turn of the worker. Table 3 summarizes three groups of experiment results, including the path length. Path length means the length from the starting point to the target point, including locally planned paths.

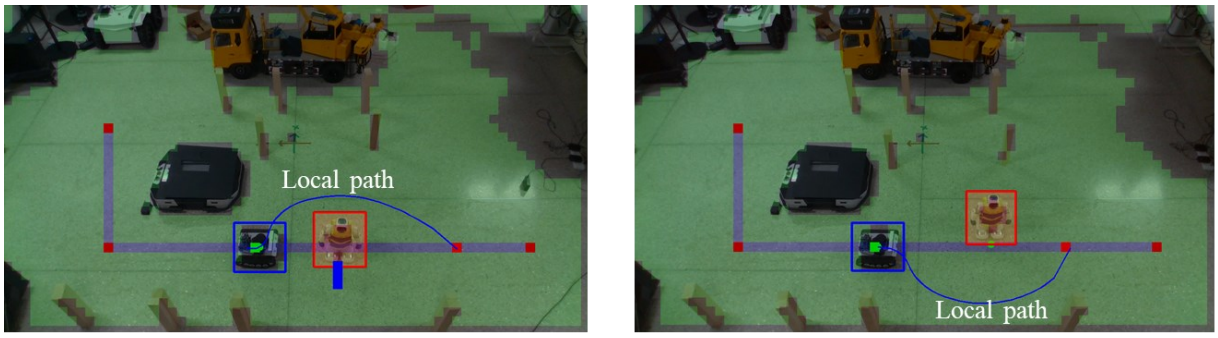

(a) Dynamic planning with the predicted trajectory (b) Dynamic planning without the predicted trajectory

Figure 7. The improved DWA

Table 1. Comparison of traditional and improved A*

Experiment	1	2	3
Time for traditional A* (s)	38.27	30.46	31.32
Time for improved A* (s)	13.05	12.96	11.42

Table 2. Comparison of prediction results for the worker and decisions for the robot

Experiment		1	2	3
Without a sudden turn	Predicted results	Success	Success	Success
	Decision for the robot	(2)	(3)	(1)
With a sudden turn	Predicted results	Failure	Failure	Failure
	Decision for the robot	(2)	(2)	(2)

Table 3. Comparison of traditional and improved DWA

Experiment	Path length (m)		Reduced weight of paths (%)
	Traditional DWA	Improved DWA	
1	5.41	4.97	8.1
2	5.49	5.01	8.7
3	6.04	5.17	14.4

4.3 Discussion

The results indicate that the construction robot can reach the target point by avoiding the moving workers, ensuring path safety. According to Table 1, the improved A* can enhance the efficiency of global planning. After fusing the safe space and the predicted worker trajectory, the improved DWA algorithm can find the path behind the worker, avoiding multiple planning and secondary collisions with the worker (see Figure. 7). The improvement further ensures path safety and path planning efficiency. Table 2 illustrates that the method can successfully predict the worker's trajectory without a sudden turn, while a sudden turn by a worker may lead to failed predictions. In the case of failed predictions, the decision model will make the robot decelerate to avoid the collision.

According to Table 3, the improved method can achieve a shorter path, 8% less than the traditional A* and DWA methods. Meanwhile, the decision model can avoid unnecessary local planning, making the planning process more efficient. For example, although the robot and worker paths overlap in Figure. 6, they arrive at the PCZ at different times, which means there is no collision between them and no need for local path replanning.

5 Conclusion

This research proposes a construction robot path planning method to cope with the dynamic environment at construction sites. Specifically, a grid map incorporating a construction schedule is established, an improved A* is developed for global path planning, the safe space and worker trajectory prediction are considered to improve the DWA algorithm for local path planning, and a decision model is developed to enhance efficiency in local path planning. It is shown from the experiment that 1) the proposed method can find a global path efficiently, 2) the improved DWA can generate a safe path, avoiding secondary collisions with the worker, and 3) the decision model reduces robot local path replanning and better maintains globally optimal paths. Thus, the proposed method can effectively support construction robot path planning at construction sites.

The limitations of this research are summarized as well. Firstly, the experiment tests are conducted in a laboratory environment, which ignores some unpredictable disturbances. Secondly, only one worker and one robot are considered in this research. Future research will conduct experiments in the field and consider other disturbances, such as multiple robots, faster worker speeds and temporary piles of material.

Acknowledgment

We would like to thank the National Natural Science Foundation of China (Grant No. 52278310, 51578318) for supporting this research.

References

[1] Bock T. The future of construction automation: technological disruption and the upcoming ubiquity of robotics. *Automation in Construction*, 59: 113–121, 2015.

[2] Barbosa F., Mischke J., Parsons M. Improving construction productivity. On-line: https://www.mckinsey.com/capabilities/operations/our-insights/improving-construction-productivity, Accessed: 18/07/2017.

[3] Cai S., Ma Z., Skibniewski M.J. *et al.* Construction automation and robotics for high-rise buildings over the past decades: A comprehensive review. *Advanced Engineering Informatics*, 42: 100989, 2019.

[4] Ding L., Jiang W., Zhou Y. *et al.* BIM-based task-level planning for robotic brick assembly through image-based 3D modeling. *Advanced Engineering Informatics*, 43: 100993, 2020.

[5] Wang Z., Li H., Zhang X. Construction waste recycling robot for nails and screws: computer vision technology and neural network approach. *Automation in Construction*, 97: 220–228, 2019.

[6] Soltani A.R., Tawfik H., Goulermas J.Y. *et al.* Path planning in construction sites: performance evaluation of the Dijkstra, A∗, and GA search algorithms. *Advanced Engineering Informatics*, 16(4): 291–303, 2002.

[7] Wang B., Liu Z., Li Q. *et al.* Mobile robot path planning in dynamic environments through globally guided reinforcement learning. In *IEEE Robotics and Automation Letters*, pages 6932–6939, 2020.

[8] Pinto A.M., Moreira E., Lima J. *et al.* A cable-driven robot for architectural constructions: a visual-guided approach for motion control and path-planning. *Autonomous Robots*, 41(7): 1487–1499, 2017.

[9] Do H., Veerajagadeshwar P., Sun F. *et al.* Combined grid and heat conduction optimization for staircase cleaning robot path planning. *Automation in Construction*, 141: 104447, 2022.

[10] Chen Z., Chen K., Song C. *et al.* Global path planning based on BIM and physics engine for UGVs in indoor environments. *Automation in Construction*, 139: 104263, 2022.

[11] Stentz A. Optimal and efficient path planning for partially-known environments. In *Proceedings of the 1994 IEEE International Conference on Robotics and Automation*, pages 3310–3317, 2014.

[12] Ali M.S.A.D., Babu N.R., Varghese K. Collision free path planning of cooperative crane manipulators using genetic algorithm. *Journal of Computing in Civil Engineering*, 19(2): 182–193, 2005.

[13] Yu L., Huang M.M., Jiang S. *et al.* Unmanned aircraft path planning for construction safety inspections. *Automation in Construction*, 154: 105005, 2023.

[14] Duchoň F., Babinec A., Kajan M. *et al.* Path planning with modified A star algorithm for a mobile robot. *Procedia Engineering*, 96: 59–69, 2014.

[15] Chen Y., Yu J., Su X. *et al.* Path planning for multi-UAV formation. *Journal of Intelligent & Robotic Systems*, 77(1): 229–246, 2015.

[16] Xu C., Liu J., Wu Z. *et al.* Automated steel reinforcement detailing in reinforced concrete frames using evolutionary optimization and artificial potential field. *Automation in Construction*, 138: 104224, 2022.

[17] Krishna Lakshmanan A., Elara Mohan R., Ramalingam B. *et al.* Complete coverage path planning using reinforcement learning for Tetromino based cleaning and maintenance robot. *Automation in Construction*, 112: 103078, 2020.

[18] Cai J., Du A., Liang X. *et al.* Prediction-based path

planning for safe and efficient human–robot Collaboration in Construction via Deep Reinforcement Learning. *Journal of Computing in Civil Engineering*, 37(1): 04022046, 2023.

[19] Zhang W., Wang N., Wu W. A hybrid path planning algorithm considering AUV dynamic constraints based on improved A* algorithm and APF algorithm. *Ocean Engineering*, 285: 115333, 2023.

[20] Duan P., Zhou J., Goh Y.M. Spatial-temporal analysis of safety risks in trajectories of construction workers based on complex network theory. *Advanced Engineering Informatics*, 56: 101990, 2023.

[21] Rao A.S., Radanovic M., Liu Y. *et al.* Real-time monitoring of construction sites: sensors, methods, and applications. *Automation in Construction*, 136: 104099, 2022.

[22] Rudenko A., Palmieri L., Herman M. *et al.* Human motion trajectory prediction: a survey. *The International Journal of Robotics Research*, 39(8): 895–935, 2020.

[23] Zhu Z., Park M.-W., Koch C. *et al.* Predicting movements of onsite workers and mobile equipment for enhancing construction site safety. *Automation in Construction*, 68: 95–101, 2016.

[24] Rashid K.M., Behzadan A.H. Risk behavior-based trajectory prediction for construction site safety monitoring. *Journal of Construction Engineering and Management*, 144(2): 04017106, 2018.

[25] Arslan M., Cruz C., Ginhac D. Semantic trajectory insights for worker safety in dynamic environments. *Automation in Construction*, 106: 102854, 2019.

[26] Tang S., Golparvar-fard M., Naphade M. *et al.* Video-based activity forecasting for construction safety monitoring use cases. In *Computing in Civil Engineering 2019*, pages 204–210, 2019.

[27] Tang S., Golparvar-Fard M., Naphade M. *et al.* Video-based motion trajectory forecasting method for proactive construction safety monitoring Systems. *Journal of Computing in Civil Engineering*, 34(6): 04020041, 2020.

[28] Cai J., Zhang Y., Yang L. *et al.* A context-augmented deep learning approach for worker trajectory prediction on unstructured and dynamic construction sites. *Advanced Engineering Informatics*, 46: 101173, 2020.

[29] Guo H., Ye X., Ren Q. *et al.* Automatic generation of construction schedules based on BIM and rule reasoning. *Journal of Tsinghua University*, 62(2): 189–198, 2022.

[30] The State Bureau of Quality and Technical Supervision. GB/T 13547-92 Human dimensions in workspace, China, 1992.

[31] International Organization for Standardization. ISO/TS 15066 Robots and robotic devices-collaborative robots, Switzerland, 2016.

[32] International Organization for Standardization. ISO 13855 Safe of machinery – Positioning of safeguards with respect to the approach speeds of parts of human body, Switzerland, 2010.

[33] International Organization for Standardization. ISO 10218-2 Robots and robotic devices-safety requirements for industrial robots-part 2: robots systems and integration, Switzerland, 2011.

[34] Arasaratnam I., Haykin S. Cubature kalman filters. *IEEE Transactions on Automatic Control*, 54(6): 1254–1269, 2009.